

RESEARCH ARTICLE | OCTOBER 23 2024

Nucleation and phase transition of decagonal quasicrystals



Tiejun Zhou ; Lei Zhang ; Pingwen Zhang ; An-Chang Shi ; Kai Jiang



J. Chem. Phys. 161, 164503 (2024)

<https://doi.org/10.1063/5.0232334>



Articles You May Be Interested In

Phase ordering of hard needles on a quasicrystalline substrate

J. Chem. Phys. (May 2012)

Clustering and mobility of hard rods in a quasicrystalline substrate potential

J. Chem. Phys. (December 2012)

Programming patchy particles to form three-dimensional dodecagonal quasicrystals

J. Chem. Phys. (May 2021)



The Journal of Chemical Physics

Special Topics Open for Submissions

[Learn More](#)

Nucleation and phase transition of decagonal quasicrystals

Cite as: J. Chem. Phys. 161, 164503 (2024); doi: 10.1063/5.0232334

Submitted: 6 August 2024 • Accepted: 9 October 2024 •

Published Online: 23 October 2024



View Online



Export Citation



CrossMark

Tiejun Zhou,¹ Lei Zhang,^{2,a)} Pingwen Zhang,^{3,4,b)} An-Chang Shi,^{5,c)} and Kai Jiang^{1,d)}

AFFILIATIONS

¹Hunan Key Laboratory for Computation and Simulation in Science and Engineering, Key Laboratory of Intelligent Computing and Information Processing of Ministry of Education, School of Mathematics and Computational Science, Xiangtan University, Xiangtan, Hunan 41105, China

²Beijing International Center for Mathematical Research, Peking University, Beijing 100871, China

³School of Mathematics and Statistics, Wuhan University, Wuhan 430072, China

⁴School of Mathematical Sciences, Peking University, Beijing 100871, China

⁵Department of Physics and Astronomy, McMaster University, Hamilton, Ontario L8S 4M1, Canada

^{a)}Electronic mail: zhangl@math.pku.edu.cn

^{b)}Electronic mail: pzhang@pku.edu.cn

^{c)}Electronic mail: shi@mcmaster.ca

^{d)}Author to whom correspondence should be addressed: kaijiang@xtu.edu.cn

ABSTRACT

In this work, we study the nucleation of quasicrystals from liquid or periodic crystals by developing an efficient order–order phase transition algorithm, namely, the nullspace-preserving saddle search method. In particular, we focus on nucleation and phase transitions of the decagonal quasicrystal (DQC) based on the Lifshitz–Petrich model. We present the nucleation path of DQC from the liquid and demonstrate one- and two-stage transition paths between DQC and periodic crystals. We provide a perspective of the group–subgroup phase transition and nucleation rates to understand the nucleation and phase transition mechanisms involving DQC. These results reveal the one-step and multi-step modes of symmetry breaking or recovery in the phase transition from DQC, where the multi-step modes are more probable.

Published under an exclusive license by AIP Publishing. <https://doi.org/10.1063/5.0232334>

I. INTRODUCTION

Quasicrystals are space-filling ordered structures possessing rotational symmetry but without translational invariance. They have been a topic of significant interest in the fields of materials science and condensed matter physics since their first discovery.¹ Numerous quasicrystals with 5-, 8-, 10-, 12-, and 18-fold rotational symmetries have been reported in metallic alloys² and soft matter.^{3–5} Moreover, quasicrystals, especially decagonal quasicrystals (DQC), have been studied from various perspectives, including formation,^{6–8} geometric features,^{9,10} and thermodynamic stability.^{11–14} However, the nucleation mechanism of quasicrystals from the liquid and periodic crystals is a topic that requires close attention.¹⁵

Over the past decades, much attention has been devoted to studying the nucleation and phase transition of quasicrystals since the first discovery, but little progress has been made. Experimentally, only some snapshots of nucleation phenomena have been

observed because the nucleation events are rare and occur at ultra-high speeds.^{16–20} In particular, the critical nuclei of quasicrystals usually possess very high surface energies and are extremely unstable, existing for very short time. It is difficult to capture the critical nuclei and the kinetic process of quasicrystal nucleation due to the lack of precise characterization techniques. Theoretical studies could provide an effective way to study nucleation and phase transition. Several mainstream theoretical frameworks include atomistic simulations,²¹ density functional theories,²² and Landau theories.²³ These theories have been successfully applied to study nucleation and phase transition of the liquid, periodic crystals, and liquid crystals.^{24–27} However, in the case of quasicrystals, previous studies have focused on studying the growth of quasicrystals by imposing initial embryos.^{28–32} The spontaneous nucleation of quasicrystals has rarely been reported and remains a challenge in simulation, limited by the computational methods to locate critical nuclei.

Theoretically, the key to studying nucleation is to find the index-1 saddle points (transition states and critical nuclei) on the free energy landscape. Ordered phases, such as quasicrystals and periodic crystals, usually correspond to degenerate local minima whose Hessian has a nullspace. When searching for a transition state from a degenerate local minimum, the presence of nullspaces makes escaping from the basin very difficult. Furthermore, since quasicrystals and crystals are incommensurate, there are no obvious epitaxial relations between them. How to represent quasicrystals and crystals in the same computational framework also increases the difficulties in theory. Thus, designing suitable methods for degenerate saddle search problems has long been an important issue. In recent years, two effective saddle search methods for degenerate saddle search problems have been proposed, including the high-index saddle dynamics method^{33,34} and the nullspace-preserving saddle search (NPSS) method.³⁵ The former escapes the basin by climbing along an ascent space that includes the nullspace and an ascent direction, while the latter climbs upward along an ascent direction orthogonal to the nullspace of the initial states. These studies have offered efficient methods to study the nucleations and phase transitions of the quasicrystals. Based on these two methods, the transition paths of the dodecagonal quasicrystal have been revealed.^{34,35} However, for the DQC, its nucleation and transition mechanisms are still unclear. For example, what structures can undergo phase transitions to or from DQC? What intermediate states are involved? How does the symmetry transform?

In this work, we focus on the study of nucleation and phase transitions involving DQC based on the Lifshitz–Petrich (LP) model. In particular, we identify three new ordered phases based on the symmetry of DQC, including the fusiform crystal (FC), pseudo-sixfold crystal (PC6), and lamellar quasicrystal (LQ). Using the NPSS method, we obtain transition states and minimum energy paths (MEPs) representing the most probable transition paths between different stable phases. We show the nucleation path of DQC from the liquid and find two transient structures,^{36,37} HEX-like and LQ-like, which benefit the formation of nuclei. We also demonstrate

one- and two-stage transition paths between DQC and crystals. We analyze these phase transitions with the group–subgroup phase transition theory³⁸ and nucleation rates. These results reveal that the phase transition from DQC could follow one-step and multi-step modes of symmetry breaking or recovery, where the multi-step modes of breaking or recovery are easier to occur.

II. THEORETICAL FRAMEWORK

A. The Lifshitz–Petrich model

The LP model provides a useful framework for characterizing the phases and phase transitions of quasiperiodic systems, including the bifrequency excited Faraday wave¹² and soft-matter quasicrystals.^{39,40} The LP model introduces a scalar order parameter $\psi(\mathbf{r})$ to represent the density profile in a domain Ω . The LP free energy is

$$\mathcal{F}_{LP}(\psi) = \int_{\Omega} \left\{ \frac{1}{2} [(1^2 + \Delta)(q^2 + \Delta)\psi]^2 - \frac{\tau}{2} \psi^2 - \frac{\gamma}{3} \psi^3 + \frac{1}{4} \psi^4 \right\} d\mathbf{r}, \quad (1)$$

where τ is a temperature-like controlling parameter and γ characterizes the intensity of three-body interaction.^{40,41} Here, 1 and q are two characteristic length scales, which are needed to stabilize the quasicrystals. Furthermore, we impose the mean zero condition of order parameter on the LP systems to ensure the mass conservation $\int_{\Omega} \psi(\mathbf{r}) d\mathbf{r} = 0$, which comes from the definition of the order parameter, i.e., the deviation from average density.

In this work, we study the nucleation and phase transition of two-dimensional DQC based on the LP model. To stabilize the DQC, the second length scale q is selected as $2 \cos(\pi/5)$ as dictated by the tenfold symmetry.⁴⁰ Figures 1(a)–1(d) show four ordered structures associated with tenfold symmetry in physical and reciprocal spaces, including DQC, PC6, FC, and LQ phases. FC and PC6 are new periodic crystals obtained by locating a set of major diffraction spectra forming a parallelogram with the central point in the reciprocal space. Their reciprocal lattice vectors (RLVs) are linear

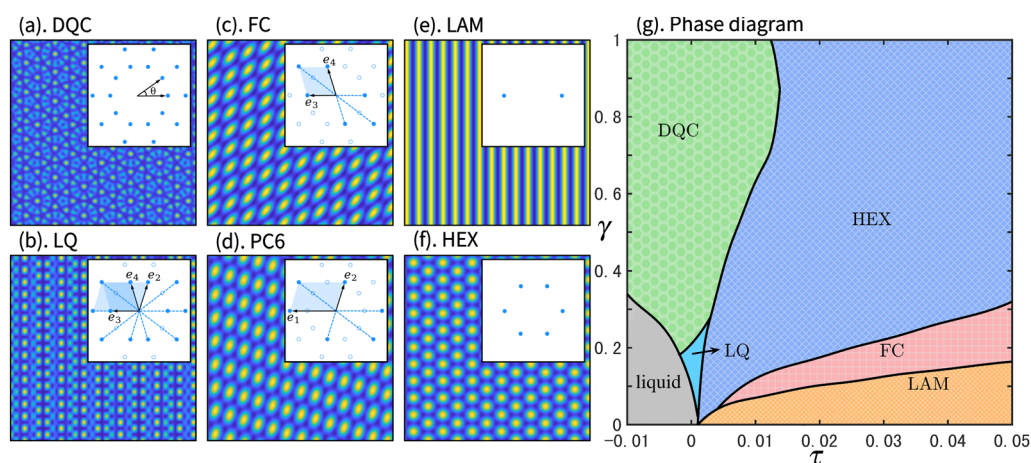


FIG. 1. Ordered structures (a)–(f) and phase diagram (g) of the LP model with $q = 2 \cos(\pi/5)$. (a) DQC; (b) LQ; (c) FC; (d) PC6; (e) LAM; and (f) HEX. Panels (b)–(d) are the new structures associated with tenfold symmetry, where the hollow points represent the corresponding positions of major diffraction spectra of DQC, and the solid points are the major diffraction spectra of new structures. PC6 is metastable in the phase diagram (g).

combinations of basic vectors $\{e_1, e_2\}$ and $\{e_3, e_4\}$ with integer coefficients, respectively, as shown in Figs. 1(c) and 1(d). LQ is a new one-dimensional quasicrystal identified by spanning the basic vectors of PC6 and FC, where $\{e_2, e_3, e_4\}$ is the linearly independent basis over the rational number field.

We construct the phase diagram in the $\tau - \gamma$ plane using an open software AGPD,⁴² which can quickly search for stable states using efficient numerical methods, such as the adaptive accelerated Bregman proximal gradient methods.^{43,44} The candidate phases that we considered include three common crystal, lamella (LAM), square, and hexagonal (HEX) phases, and four structures related to tenfold rotational symmetry: PC6, FC, LQ, and DQC. We give the initial configurations of these ordered structures in the reciprocal space and obtain the converged states when $\|\nabla\mathcal{F}\|_\infty < 10^{-11}$, where $\|(x_1, x_2, \dots, x_n)\|_\infty = \max(|x_1|, |x_2|, \dots, |x_n|)$. By comparing their energy, we call the state with the lowest energy as the stable or equilibrium state. Figures 1(a)–1(f) show five stable states in the phase diagram and one metastable state PC6 involved in phase transitions. Figure 1(g) shows the phase diagram of the LP model with $q = 2 \cos(\pi/5)$.

B. Incommensurate epitaxies

One bottleneck in studying phase transitions is that quasicrystals and crystals are incommensurate, i.e., their lattice mismatch.⁴⁵ In the case of the two-dimensional DQC, whose major RLVs are shown in Fig. 2, it is impossible to represent all its RLVs linearly using two noncollinear bases over the rational number field.

Methods to solve the lattice mismatch problem between crystals and quasicrystals include the projection method⁴⁶ and the periodic approximation method.^{47–50} The former simulates the quasiperiodic structure in a higher-dimensional periodic system, while the latter approximates the quasiperiodic structure with a periodic approximant. In this paper, we use the periodic approximation method to study phase transitions about DQC. In the computation, some RLVs are linear combinations of primitive RLVs with irrational coefficients, which are difficult for the current computers to store. For the irrational number κ , we can approximate it with the rational

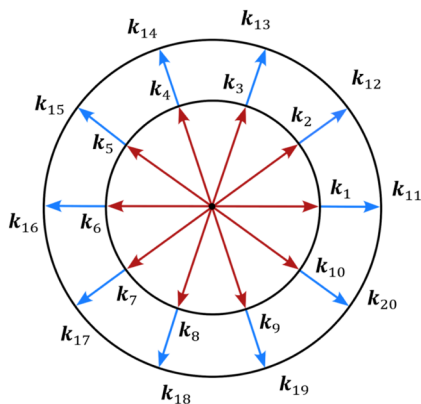


FIG. 2. RLVs of two-dimensional DQC, where $k_j = [\cos(j\pi/5), \sin(j\pi/5)]$ for $j = 1, 2, \dots, 10$, and $k_j = [q \cos(j\pi/5), q \sin(j\pi/5)]$ for $j = 11, 12, \dots, 20$.

TABLE I. Coefficients of RLVs for DQC required to be approximated simultaneously.

$ k = 1$	1,	$\cos(\pi/5)$,	$\sin(\pi/5)$,	$\sin(2\pi/5)$,	$\cos(2\pi/5)$
$ k = q$	q ,	$q \cos(\pi/5)$,	$q \sin(\pi/5)$,	$q \sin(2\pi/5)$,	$q \cos(2\pi/5)$

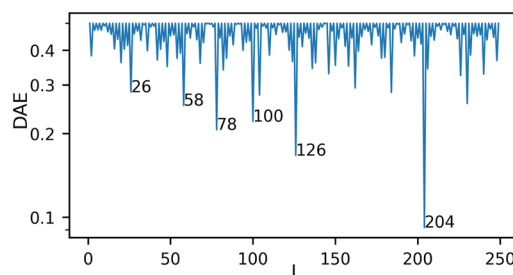


FIG. 3. DAE of different computational domain sizes $[0, 2\pi L]^2$ for studying the phase transitions involving two-dimensional DQC.

number $[L\kappa]$, where $[a]$ rounds a to the nearest integer. Applying Diophantine approximation theory, the proper value L satisfying the required accuracy can be determined by the Diophantine approximation error (DAE).⁵¹ Then, the quasiperiodic structure can be approximated by the periodic structure in a finite domain with the period $[0, 2\pi L]^2$. For two primitive RLVs, $e_1^* = (1, 0)$ and $e_2^* = (0, 1)$, the coefficients of RLVs about DQC required to be approximated simultaneously are presented in Table I.

Figure 3 shows the DAEs as the integer L increases.^{34,46,51} In this work, we select $L = 126$ ($DAE = 0.167$) and $L = 204$ ($DAE = 0.092$) to obtain the proper computational domains, which can encompass the critical nucleus in the phase transition.

C. Nullspace-preserving saddle search method

Quasicrystals can be embedded into high-dimensional periodic systems and can thus be viewed as having translational invariance in superspace. For the energy functional (1), critical points (local minima/maxima, saddle points) characterizing DQC and its symmetry-related ordered structures are usually degenerate.^{34,44} For a degenerate local minima ψ_0 , its Hessian $H(\psi_0) = \nabla^2\mathcal{F}(\psi_0)$ usually has a nullspace. The dimension k of the nullspace usually indicates that the corresponding ordered structure is inhomogeneous periodic in the k -dimensional space.^{35,44} The presence of the nullspace may prevent escape from the attraction basin of ψ_0 because the eigenvectors corresponding to zero eigenvalues would be mistaken as the ascent direction.

The NPSS method is an efficient saddle search method for ordered phase transitions, which can escape from the basin quickly by exploiting the properties of nullspaces and symmetry-breaking.³⁵ In particular, at a degenerate state ψ in the attraction basin of ψ_0 , keeping the ascent direction v orthogonal to the nullspace $\mathcal{W}^k(\psi)$ can eliminate the effects of nullspace. To avoid computing the nullspace at each iteration, the NPSS method uses the nullspace $\mathcal{W}^k(\tilde{\psi})$ of the initial state $\tilde{\psi} = \psi_0$ to replace that of ψ . Then, the NPSS keeps the ascent direction v orthogonal to the nullspace $\mathcal{W}^k(\tilde{\psi})$.

When the difference between nullspaces of the current and initial states becomes distinct, we update $\tilde{\psi} = \psi$ and continue to climb as above. These operations ensure the effectiveness of the ascent direction and reduce the costs of updating the nullspaces. Therefore, the NPSS method updates the state ψ by

$$\beta^{-1}\dot{\psi} = -\mathcal{P}_{\mathcal{V}}T(\psi) + (I - \mathcal{P}_{\mathcal{V}})T(\psi), \quad (2)$$

where $T(\psi) = -\nabla\mathcal{F}(\psi)$ is the negative gradient and β represents the positive relaxation constant. $\mathcal{P}_{\mathcal{V}}$ denotes the orthogonal projection operator onto the subspace \mathcal{V} . Furthermore, the ascent direction v can be updated by

$$\xi^{-1}\dot{v} = -H(\psi)v + \langle v, H(\psi)v \rangle v + 2\sum_{i=1}^{l_k} \langle \tilde{v}_i^k, H(\psi)v \rangle \tilde{v}_i^k, \quad (3)$$

where $\xi > 0$ are the relaxation parameters, v satisfies the unitization constraint, and $\{\tilde{v}_i^k\}_{i=1}^{l_k}$ are basic vectors of $\mathcal{W}^k(\tilde{\psi})$.

As ψ climbs upward on the potential energy surface, updating v is no longer affected by the nullspace after the smallest eigenvalue of $H(\psi)$ becomes negative. Thus, we update v by

$$\xi^{-1}\dot{v} = -H(\psi)v + \langle v, H(\psi)v \rangle v, \quad (4)$$

This NPSS method has shown its superiority in studying the phase transition of crystals and dodecagonal quasicrystals with an economical computational. Numerical details can be found in a previous work.³⁵

III. RESULTS AND DISCUSSION

A. Nucleation of DQC from liquid

In this subsection, we investigate the nucleation of DQC from the liquid state. We select an appropriate computational domain $\Omega = [0, 2\pi L]^2$ with $L = 126$ and spatial discretization points $N = 1024$ in each dimension. For $\tau = -0.01$ and $\gamma = 0.5$ in the LP model (1), DQC is the stable state with a free energy density of $f = \mathcal{F}/|\Omega| = -8.96 \times 10^{-5}$, while the liquid is metastable with $f = 0$. As shown in Fig. 4(a), we obtain the critical nucleus of DQC with $f = 2.38 \times 10^{-8}$ by using the NPSS method, which represents the transition state on the MEP.

On the MEP, the liquid is an isotropic high-symmetry phase whose all symmetry operations belong to the extended Euclidean space group $E(\mathbb{R}^2)$.³⁸ DQC has no translational invariance but a tenfold rotation symmetry and two mutually exclusive mirror symmetries. Thus, DQC is a low-symmetry phase with space group $p10$ mm in comparison with the liquid.⁵² Obviously, $p10$ mm is a subgroup of $E(\mathbb{R}^2)$, and a group-subgroup phase transition from the high-symmetry phase to the low-symmetry phase occurs by symmetry breaking. From the diffraction patterns shown in Fig. 4(b), the diffraction spectra cluster of the critical nucleus starts to show an incomplete tenfold symmetry, indicating that the symmetry of the original structure is broken and a new symmetric structure is forming. Due to the presence of energy barriers, the appearance and initial growth of the nucleus is thermodynamically unfavorable. When the size of the DQC nucleus is smaller than that of the critical nucleus, the nucleus tends to disappear. After the DQC nucleus attains a critical size, its growth becomes

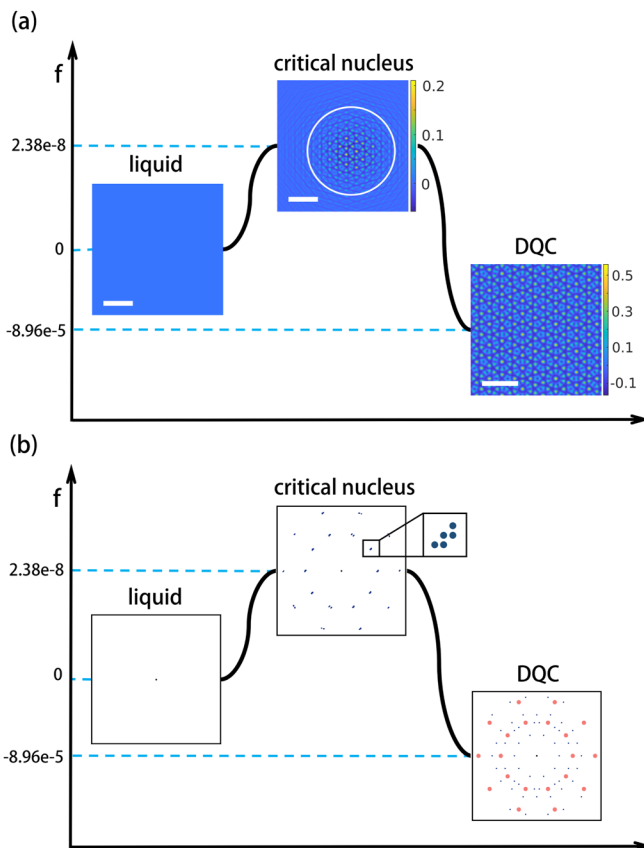


FIG. 4. (a). Transition path from liquid to DQC computed by using the NPSS method in the LP model with $\tau = -0.01$ and $\gamma = 0.5$, where $L = 126$ and $N = 1024$. All the white scale bars present 10π . (b). Diffraction spectra of stationary points on the transition path from liquid to DQC as shown in panel (a). The major diffraction spectra are labeled in salmon color, and the minor diffraction spectra are labeled in blue.

thermodynamically favorable and the nucleus will grow irreversibly, thus completely transforming into the DQC.

Furthermore, it is interesting that two transient structures, HEX-like and LQ-like, are found in the nucleation process, as shown in Fig. 5(a). First, a localized HEX-like structure emerges in the amorphous phase. As the DQC nucleus becomes gradually visible, the LQ-like structure appears as a bridging phase at the boundary between the DQC and amorphous or HEX-like phases. Once the critical nucleus forms, both the HEX-like and LQ-like transient structures disappear. During the growth process, an LQ-like phase also exists in the marginal regions of the DQC nucleus, as shown in Fig. 5(b). These transient structures are unstable and vanish finally, serving to construct the disorder-order connections.³¹ In particular, they might be favorable for the formation of critical nuclei during the nucleation process.

B. Phase transition from DQC to FC

We study how FC emerges from DQC. At $\tau = 0.018$ and $\gamma = 0.4$ in the LP model, we obtain several paths for the phase transition

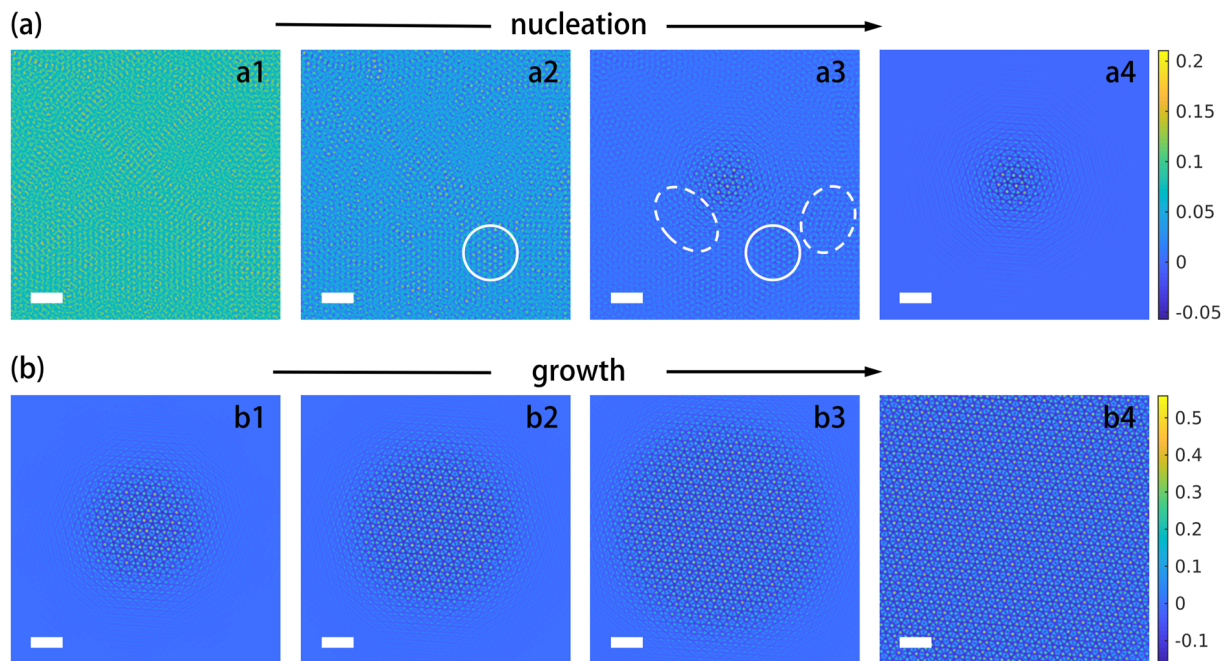


FIG. 5. Snapshots on nucleation (a) and growth (b) processes of transition path from liquid to DQC shown in Fig. 4. The white solid circles in (a2) and (a3) show the HEX-like transient structures, and the white dash circles in (a3) present the LQ-like transient structures. In panels (b1)–(b3), the LQ-like transient structure also exists in the marginal regions of the DQC nucleus. All the white scale bars present 10π . All the figures in panels (a) and (b) share a common colour bar, respectively.

from DQC to FC through the NPSS method. As shown in Fig. 6, FC with $f = -2.85 \times 10^{-4}$ is more stable than the metastable state DQC with $f = -2.48 \times 10^{-4}$. The space group of FC is $p2$, which is a subgroup of $p10$ mm corresponding to DQC.⁵³ We observe a one-stage transition path from DQC to FC through Saddle-1 with an energy barrier $\Delta f = 2 \times 10^{-7}$. This transition follows a one-step symmetry breaking mode ($p10$ mm $\rightarrow p2$) by breaking both rotational and mirror symmetries. We then identify a metastable intermediate state LQ with the space group $p2$ mm between DQC and FC. We discover a two-stage transition path DQC \rightarrow LQ \rightarrow FC via the Saddle-2 and Saddle-4. Nucleation at the first stage transition from DQC to LQ shows an ellipsoidal critical nucleus of LQ with $\Delta f = 1 \times 10^{-7}$. From Fig. 6(b), the group-subgroup phase transition from DQC reserves mirror symmetry and breaks tenfold rotational symmetry. Consequently, LQ has a twofold rotational symmetry and two mutually perpendicular mirror symmetries along with horizontal and vertical axes. The second stage transition from LQ to FC involves the formation of another ellipsoidal critical nucleus of FC with $\Delta f = 3 \times 10^{-8}$. Since two mirror symmetries along the horizontal and vertical axes are broken, the space group eventually becomes $p2$. Compared to the one-stage transition, the two-stage transition with a multi-step symmetry-breaking mode ($p10$ mm $\rightarrow p2$ mm $\rightarrow p2$) needs to cross a lower energy barrier. It also has a higher probability of occurrence due to fewer symmetry variations at each step.

We also observe another low-symmetry phase PC6 with the space group $p2$. PC6 also has twofold rotational symmetry, but its lattice size with the edge length ratio $1 : 2 \cos(\pi/5)$ is different from that of FC with the ratio $1 : 1$. Then, we discover another two-stage

phase transition path DQC \rightarrow LQ \rightarrow PC6, which also satisfies the multi-step symmetry-breaking mode ($p10$ mm $\rightarrow p2$ mm $\rightarrow p2$). By observing the diffraction spectra shown in Fig. 6(b), we can find that FC and PC6 are transformed from LQ via two different symmetry-breaking modes, respectively. In particular, these two low-symmetry phases PC6 and FC are also connected by a special crystal-crystal phase transition. First, the symmetries are recovered to incomplete $p2$ mm, as shown by the diffraction spectrum clusters at Saddle-5 in Fig. 6(b). Then, the recovered symmetries are broken to form FC. In this process, a higher energy barrier $\Delta f = 4 \times 10^{-6}$ exists compared to other paths only with symmetry breaking. Possible causes include a high change in overall symmetry, as well as the simultaneous occurrence of symmetry breaking and recovery.

Furthermore, we estimate the nucleation rate J by the formula (5),^{26,54–57}

$$J = J_0 \exp(-\alpha \Delta f_{LP}), \quad (5)$$

where Δf_{LP} represents the dimensionless energy barrier in the LP model and $J_0 > 0$ is the kinetic prefactor. In addition, α is a dimensionless factor dependent on the concrete problem. For example, consider the block copolymer systems;⁵⁸ the difference of free energy per chain among different ordered structures is $10^{-3} \sim 10^{-2} k_B T$ through the self-consistent field theory (SCFT),⁵⁹ where k_B is the Boltzmann constant and T is the absolute temperature. If we use the LP model to study the self-assembly of block copolymers, α can be determined by comparing the energies or energy difference among different ordered structures obtained from the LP model and SCFT

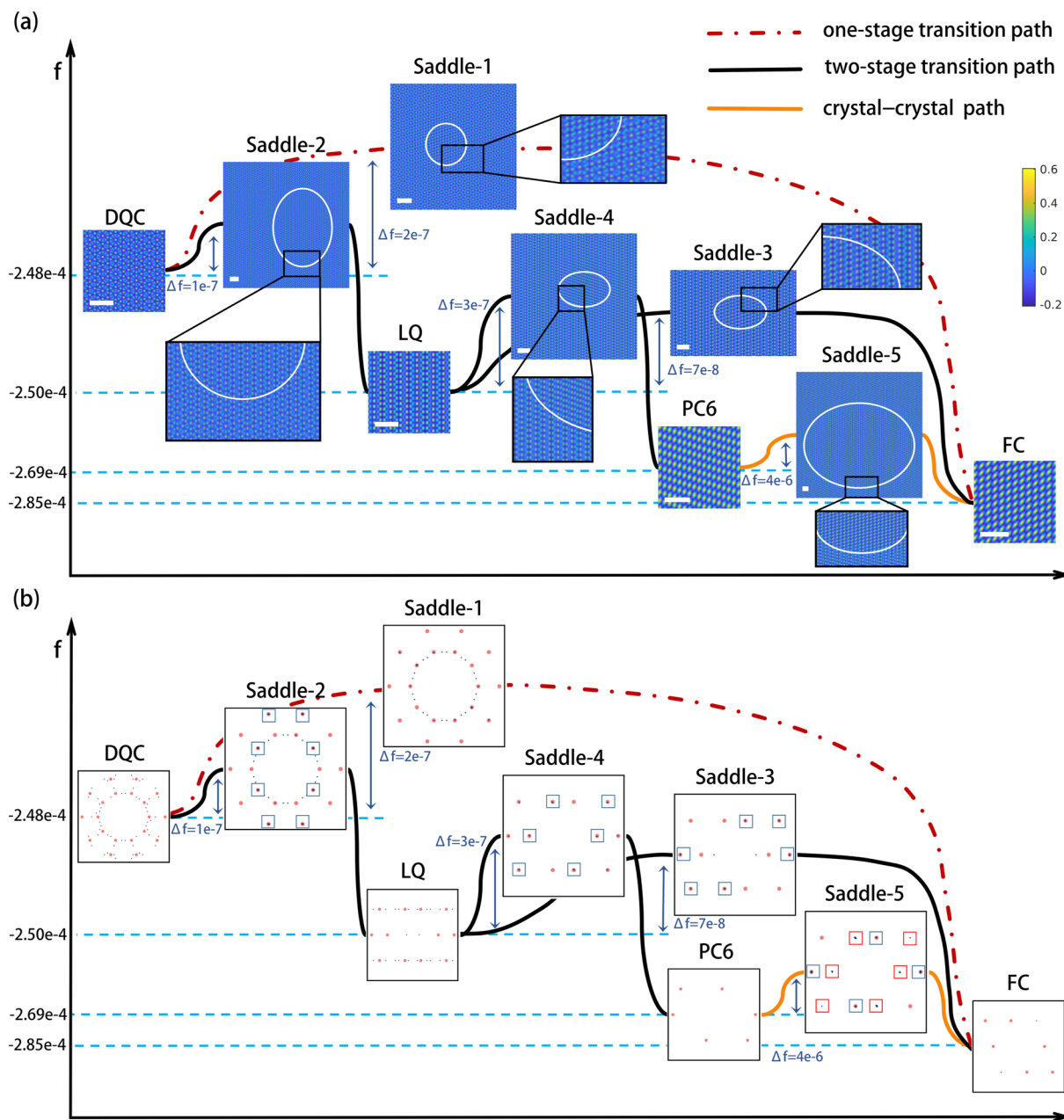


FIG. 6. (a). Transition path about DQC computed by using the NPSS method in the LP model with $\tau = 0.018$ and $\gamma = 0.4$, where $L = 126$ and $N = 1024$. Saddle- i ($i = 1, 2, \dots, 5$) are transition states on MEPs. All the white scale bars present 10π , and all the figures share a common colour bar. (b) Diffraction spectra of stationary points on the transition path from DQC to FC as shown in panel (a) The blue and red boxes mark the diffraction spectra changed in symmetry breaking and recovery, respectively.

model. Here, in the nucleation process, the nucleation rate is only dominated by the energy barrier Δf . From (5), it is easy to find that the nucleation rates from DQC to Saddle-2 and LQ to Saddle-3 are higher. This also indicates that the transition with a multi-step symmetry breaking is more likely than the transition with a one-step symmetry breaking.

C. Phase transition from FC to DQC

In this subsection, we explore the multi-step emergence of DQC from FC. By selecting $\tau = -1 \times 10^{-4}$ and $\gamma = 0.32$ in the LP model, we observe that FC becomes a metastable state with $f = -2.63 \times 10^{-5}$ and DQC reaches a stable state with $f = -2.99 \times 10^{-5}$. We discover a two-stage transition path $FC \rightarrow LQ \rightarrow DQC$

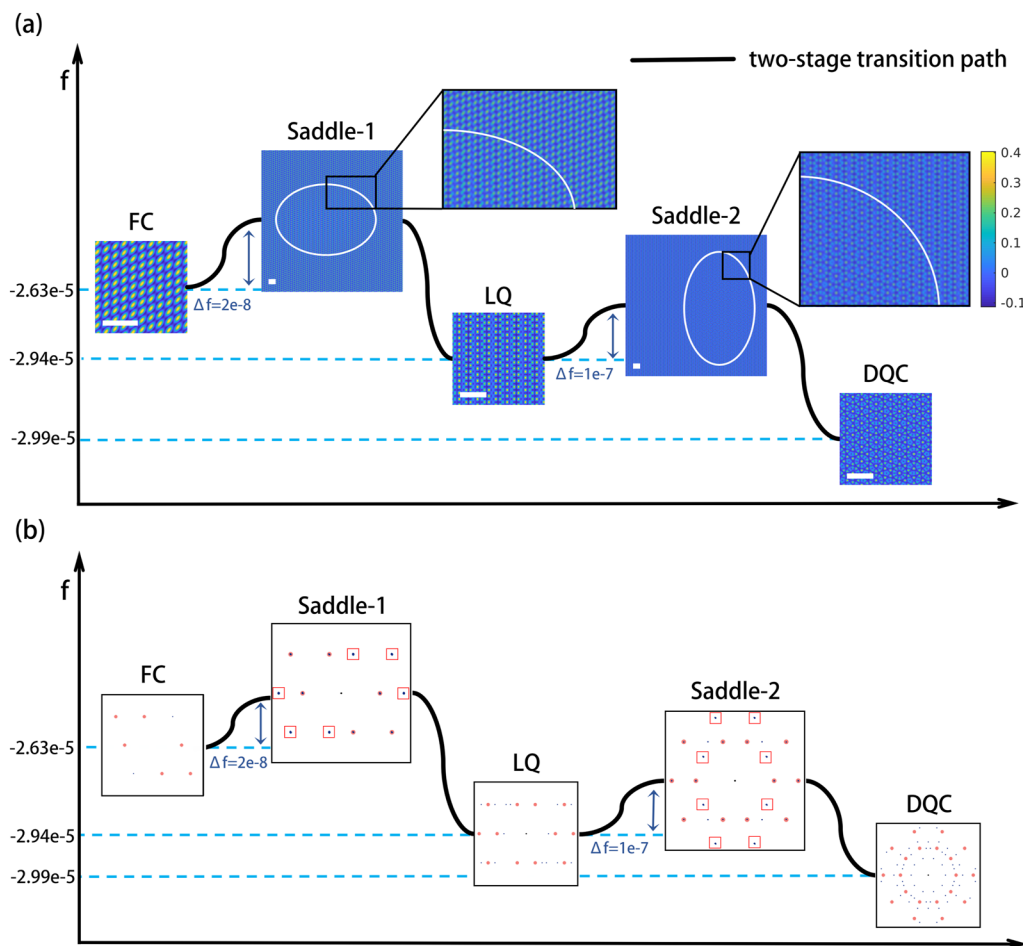


FIG. 7. (a). Transition path from FC to DQC computed by using the NPSS method in the LP model with $\tau = -1 \times 10^{-4}$ and $\gamma = 0.32$, where $L = 204$ and $N = 2048$. Saddle- i ($i = 1, 2$) are transition states on these transition paths. All the white scale bars present 10π , and all the figures share a common colour bar. (b). Diffraction spectra of stationary points on transition path from FC to DQC as shown in panel (a). The marked boxes have the same meaning as in Fig. 6.

via a metastable intermediate state, as shown in Fig. 7. Here, FC is a low-symmetry phase whose space group is a subgroup of that of DQC. The group-subgroup phase transition occurs through multi-step symmetry recovery. In the first stage, the mirror symmetries recover from $p2$ to $p2$ mm via an ellipsoidal critical nucleus of LQ, which is quasiperiodic in the major axis direction. In the second stage, the space group becomes $p10$ mm with rotational symmetry recovery, and a quasiperiodic order is formed in the remaining periodic direction. As shown in Fig. 7(b), comparing the recovered diffraction spectra in Saddle-1 and Saddle-2, a fact is revealed that a larger symmetry variation corresponds to a higher energy barrier. However, the one-stage transition from FC to DQC is not observed, perhaps because the two-stage transition path with multi-step symmetry recovery is the more likely path. Another possible reason is that the attraction basins of FC and DQC on the potential energy surface are not adjacent. Alternatively, there may be an LQ attraction basin between them. Once the system escapes the FC attraction basin, it will easily fall into the LQ attraction basin.

IV. CONCLUSIONS

In this work, we investigate the nucleation and transition pathway of DQCs by using the recently developed nullspace-preserving saddle search method,³⁵ which greatly improves the calculation efficiency of studying ordered phase transitions. We obtain the nucleation path of DQC from the liquid and the one- and two-stage transition paths between DQC and crystals. In the path from DQC to the liquid, we find two transient structures, HEX-like and LQ-like, which contribute to the construction of the disorder-order links. Furthermore, we provide a new perspective on the group theory to understand the phase transition mechanism involving quasicrystals and discuss the nucleation rate. The results reveal that the phase transitions from DQC could follow one-step and multi-step symmetry-breaking modes to two distinct low-symmetry phases, FC and PC6. Interestingly, these two low-symmetry phases can also be linked by undergoing transitions with simultaneous symmetry recovery and breaking. Then, a larger symmetry variation necessitates overcoming higher energy barriers. Meanwhile, the phase

transitions with the multi-step mode of symmetry breaking or recovery are more likely to occur. Overall, our work offers a novel and comprehensive insight into the transition pathways and mechanisms of DQC.

ACKNOWLEDGMENTS

This work was supported by the National Key R & D Program of China (Grant No. 2023YFA1008802), the National Natural Science Foundation of China (Grant Nos. 12171412 and 12288101), the Science and Technology Innovation Program of Hunan Province (Grant No. 2024RC1052), and the Innovative Research Group Project of Natural Science Foundation of Hunan Province of China (Grant No. 2024JJ1008). T.J.Z. was partially supported by the Post-graduate Scientific Research Innovation Project of Hunan Province (Grant No. CX20230631). We acknowledge the High Performance Computing Platform of Xiangtan University for the partial support of this work.

AUTHOR DECLARATIONS

Conflict of Interest

The authors have no conflicts to disclose.

Author Contributions

Tiejun Zhou: Conceptualization (equal); Data curation (equal); Formal analysis (equal); Investigation (equal); Methodology (equal); Validation (equal); Visualization (equal); Writing – original draft (equal); Writing – review & editing (equal). **Lei Zhang:** Conceptualization (equal); Methodology (equal); Supervision (equal); Validation (equal). **Pingwen Zhang:** Methodology (equal); Resources (equal); Supervision (equal); Validation (equal). **An-Chang Shi:** Formal analysis (equal); Resources (equal); Supervision (equal); Validation (equal); Writing – review & editing (equal). **Kai Jiang:** Conceptualization (equal); Formal analysis (equal); Funding acquisition (equal); Investigation (equal); Methodology (equal); Project administration (equal); Resources (equal); Supervision (equal); Validation (equal); Visualization (equal); Writing – original draft (equal); Writing – review & editing (equal).

DATA AVAILABILITY

The data that support the findings of this study are available from the corresponding authors upon reasonable request.

REFERENCES

- ¹D. Shechtman, I. Blech, D. Gratias, and J. W. Cahn, “Metallic phase with long-range orientational order and no translational symmetry,” *Phys. Rev. Lett.* **53**, 1951–1953 (1984).
- ²D. Levine and P. J. Steinhardt, “Quasicrystals. I. Definition and structure,” *Phys. Rev. B* **34**, 596–616 (1986).
- ³X. Zeng, G. Ungar, Y. Liu, V. Percec, A. E. Dulcey, and J. K. Hobbs, “Supramolecular dendritic liquid quasicrystals,” *Nature* **428**, 157–160 (2004).
- ⁴K. Hayashida, T. Dotera, A. Takano, and Y. Matsushita, “Polymeric quasicrystal: Mesoscopic quasicrystalline tiling in ABC star polymers,” *Phys. Rev. Lett.* **98**, 195502 (2007).
- ⁵C. Xiao, N. Fujita, K. Miyasaka, Y. Sakamoto, and O. Terasaki, “Dodecagonal tiling in mesoporous silica,” *Nature* **487**, 349–353 (2012).
- ⁶K. K. Fung, C. Y. Yang, Y. Q. Zhou, J. G. Zhao, W. S. Zhan, and B. G. Shen, “Icosahedrally related decagonal quasicrystal in rapidly cooled Al-14-at.-%-Fe alloy,” *Phys. Rev. Lett.* **56**, 2060–2063 (1986).
- ⁷W. Steurer, “Structural phase transitions from and to the quasicrystalline state,” *Acta Crystallogr., Sect. A: Found. Crystallogr.* **61**, 28–38 (2005).
- ⁸J.-B. Suck, M. Schreiber, and P. Häussler, *Quasicrystals: An Introduction to Structure, Physical Properties and Applications* (Springer Science & Business Media, 2013), Vol. 55.
- ⁹D. Divincenzo and P. J. Steinhardt, *Quasicrystals: The State of the Art* (World Scientific, 1991).
- ¹⁰M. V. Jaric, *Introduction to the Mathematics of Quasicrystals* (Elsevier, 2012).
- ¹¹A. Denton and H. Löwen, “Stability of colloidal quasicrystals,” *Phys. Rev. Lett.* **81**, 469 (1998).
- ¹²R. Lifshitz and D. M. Petrich, “Theoretical model for Faraday waves with multiple-frequency forcing,” *Phys. Rev. Lett.* **79**, 1261–1264 (1997).
- ¹³P. Subramanian, A. Archer, E. Knobloch, and A. M. Rucklidge, “Three-dimensional icosahedral phase field quasicrystal,” *Phys. Rev. Lett.* **117**, 075501 (2016).
- ¹⁴P. Subramanian, A. Archer, E. Knobloch, and A. M. Rucklidge, “Spatially localized quasicrystalline structures,” *New J. Phys.* **20**, 122002 (2018).
- ¹⁵S. T. Scanlon, Y. Suleymanov, C. Ash, V. Vinson, M. McCartney, J. Yeston, and S. M. Hurlley, “In other journals,” *Science* **375**, 279–280 (2022).
- ¹⁶J. Reyes-Gasga and R. Hernandez, “Nucleation of the decagonal quasicrystalline phase in Al-Cu-Co-Si thin films,” *Thin Solid Films* **220**, 172–175 (1992).
- ¹⁷J. Smerdon, J. Parle, L. Wearing, T. A. Lograsso, A. Ross, and R. McGrath, “Nucleation and growth of a quasicrystalline monolayer: Bi adsorption on the fivefold surface of i-Al₇₀Pd₂₁Mn₉,” *Phys. Rev. B* **78**, 075407 (2008).
- ¹⁸R. Kobold, W. Hornfeck, M. Kolbe, and D. Herlach, “Quasicrystal nucleation in an intermetallic glass former,” in 6th Decennial International Conference on Solidification Processing, 2017.
- ¹⁹G. Kurtuldu, K. F. Shamlaye, and J. F. Löffler, “Metastable quasicrystal-induced nucleation in a bulk glass-forming liquid,” *Proc. Natl. Acad. Sci. U. S. A.* **115**, 6123–6128 (2018).
- ²⁰D. Wang, L. Peng, and C. M. Gourlay, “Al-Mn-based decagonal quasicrystal in AZ magnesium alloys and its nucleation on Al₃Mn₅ during solidification,” *Scr. Mater.* **241**, 115886 (2024).
- ²¹D. Kashchiv, *Nucleation* (Elsevier, 2000).
- ²²J. W. Cahn and J. E. Hilliard, “Free energy of a nonuniform system. III. Nucleation in a two-component incompressible fluid,” *J. Chem. Phys.* **31**, 688–699 (1959).
- ²³R. Cowley, “Structural phase transitions I. Landau theory,” *Adv. Phys.* **29**, 1–110 (1980).
- ²⁴X. Cheng, L. Lin, W. E, P. Zhang, and A.-C. Shi, “Nucleation of ordered phases in block copolymers,” *Phys. Rev. Lett.* **104**, 148301 (2010).
- ²⁵L. Lin, X. Cheng, W. E, A.-C. Shi, and P. Zhang, “A numerical method for the study of nucleation of ordered phases,” *J. Comput. Phys.* **229**, 1797–1809 (2010).
- ²⁶T. Li, P. Zhang, and W. Zhang, “Nucleation rate calculation for the phase transition of diblock copolymers under stochastic Cahn–Hilliard dynamics,” *Multiscale Model. Simul.* **11**, 385–409 (2013).
- ²⁷A. Samanta, M. E. Tuckerman, T.-Q. Yu, and W. E, “Microscopic mechanisms of equilibrium melting of a solid,” *Science* **346**, 729–732 (2014).
- ²⁸C. Achim, M. Schmiedeberg, and H. Löwen, “Growth modes of quasicrystals,” *Phys. Rev. Lett.* **112**, 255501 (2014).
- ²⁹M. Schmiedeberg, C. Achim, J. Hielscher, S. Kapfer, and H. Löwen, “Dislocation-free growth of quasicrystals from two seeds due to additional phasonic degrees of freedom,” *Phys. Rev. E* **96**, 012602 (2017).
- ³⁰S. Tang, Z. Wang, J. Wang, K. Jiang, C. Liang, Y. Ma, W. Liu, and Y. Du, “An atomic scale study of two-dimensional quasicrystal nucleation controlled by multiple length scale interactions,” *Soft Matter* **16**, 5718–5726 (2020).
- ³¹Z. Jiang, S. Qian, N. Xu, L. He, and Y. Ni, “Growth modes of quasicrystals involving intermediate phases and a multistep behavior studied by phase field crystal model,” *Phys. Rev. Mater.* **4**, 023403 (2020).

- ³²C. Liang, K. Jiang, S. Tang, J. Wang, Y. Ma, W. Liu, and Y. Du, “Molecular-level insights into the nucleation mechanism of one-component soft matter icosahedral quasicrystal studied by phase-field crystal simulations,” *Cryst. Growth Des.* **22**, 2637–2643 (2022).
- ³³J. Yin, L. Zhang, and P. Zhang, “High-index optimization-based shrinking dimer method for finding high-index saddle points,” *SIAM J. Sci. Comput.* **41**, A3576–A3595 (2019).
- ³⁴J. Yin, K. Jiang, A.-C. Shi, P. Zhang, and L. Zhang, “Transition pathways connecting crystals and quasicrystals,” *Proc. Natl. Acad. Sci. U. S. A.* **118**, e2106230118 (2021).
- ³⁵G. Cui, K. Jiang, and T. Zhou, “An efficient saddle search method for ordered phase transitions involving translational invariance,” *Comput. Phys. Commun.* **306**, 109381 (2025).
- ³⁶A. J. Archer, A. M. Rucklidge, and E. Knobloch, “Soft-core particles freezing to form a quasicrystal and a crystal-liquid phase,” *Phys. Rev. E* **92**, 012324 (2015).
- ³⁷A. J. Archer, A. M. Rucklidge, and E. Knobloch, “Quasicrystalline order and a crystal-liquid state in a soft-core fluid,” *Phys. Rev. Lett.* **111**, 165501 (2013).
- ³⁸K. A. Gernoth, “Analytical and numerical (Monte Carlo) studies of point and space group symmetry-breaking in the liquid–solid phase transition,” *Ann. Phys.* **291**, 202–266 (2001).
- ³⁹R. Lifshitz and H. Diamant, “Soft quasicrystals—Why are they stable?,” *Philos. Mag.* **87**, 3021–3030 (2007).
- ⁴⁰K. Jiang, J. Tong, P. Zhang, and A.-C. Shi, “Stability of two-dimensional soft quasicrystals in systems with two length scales,” *Phys. Rev. E* **92**, 042159 (2015).
- ⁴¹K. Barkan, H. Diamant, and R. Lifshitz, “Stability of quasicrystals composed of soft isotropic particles,” *Phys. Rev. B* **83**, 172201 (2011).
- ⁴²K. Jiang and W. Si, “Automatically generating phase diagram,” *National Copyright Administration of the People’s Republic of China 2022SR0139033*, *GitHub—KaijiangMath/AGPD: Automatically generating phase diagram (AGPD) software*, 2022.
- ⁴³K. Jiang, W. Si, C. Chen, and C. Bao, “Efficient numerical methods for computing the stationary states of phase field crystal models,” *SIAM J. Sci. Comput.* **42**, B1350–B1377 (2020).
- ⁴⁴C. Bao, C. Chen, K. Jiang, and L. Qiu, “Convergence analysis for Bregman iterations in minimizing a class of Landau free energy functionals,” *SIAM J. Numer. Anal.* **62**, 476–499 (2024).
- ⁴⁵T. Janssen, A. Janner, A. Looijenga-Vos, and P. de Wolff, “Incommensurate and commensurate modulated structures,” *Int. Tables Crystallogr.* **100**, 907–955 (2006).
- ⁴⁶K. Jiang and P. Zhang, “Numerical methods for quasicrystals,” *J. Comput. Phys.* **256**, 428–440 (2014).
- ⁴⁷B. Dionne, M. Silber, and A. C. Skeldon, “Stability results for steady, spatially periodic planforms,” *Nonlinearity* **10**, 321 (1997).
- ⁴⁸A. M. Rucklidge and M. Silber, “Design of parametrically forced patterns and quasipatterns,” *SIAM J. Appl. Dyn. Syst.* **8**, 298–347 (2009).
- ⁴⁹A. J. Archer, T. Dotera, and A. M. Rucklidge, “Rectangle-triangle soft-matter quasicrystals with hexagonal symmetry,” *Phys. Rev. E* **106**, 044602 (2022).
- ⁵⁰P. Zhang and X. Zhang, “An efficient numerical method of Landau–Brazovskii model,” *J. Comput. Phys.* **227**, 5859–5870 (2008).
- ⁵¹H. Davenport and K. Mahler, “Simultaneous Diophantine approximation,” *Duke Math. J.* **13**, 105–111 (1946).
- ⁵²Z. Liu, H. Li, C. Fan, and W. Luo, “Necessary and sufficient elastic stability conditions in 21 quasicrystal Laue classes,” *Eur. J. Mech.-A* **65**, 30–39 (2017).
- ⁵³B. K. Vainshtein, *Fundamentals of Crystals: Symmetry, and Methods of Structural Crystallography* (Springer Science & Business Media, 2013), Vol. 1.
- ⁵⁴T. W. Heo, L. Zhang, Q. Du, and L.-Q. Chen, “Incorporating diffuse-interface nuclei in phase-field simulations,” *Scr. Mater.* **63**, 8–11 (2010).
- ⁵⁵K. Kelton and A. L. Greer, *Nucleation in Condensed Matter: Applications in Materials and Biology* (Elsevier, 2010).
- ⁵⁶E. Ruckenstein and G. Berim, *Kinetic Theory of Nucleation* (CRC Press, 2016).
- ⁵⁷T. Li, P. Zhang, and W. Zhang, “Numerical study for the nucleation of one-dimensional stochastic Cahn–Hilliard dynamics,” *Commun. Math. Sci.* **10**, 1105–1132 (2012).
- ⁵⁸G. H. Fredrickson, *The Equilibrium Theory of Inhomogeneous Polymers* (Oxford University, 2006).
- ⁵⁹W. Li and D. Gersappe, “Self-assembly of Rod–Coil diblock copolymers,” *Macromolecules* **34**, 6783–6789 (2001).